doi.org/10.52568/000555/JCSP/43.01.2021

Efficient and Reusable Silica Gel Supported Metal Ionic Liquid Catalysts for Palmitic Acid Esterification to Biodiesel

[1]Guo Yingwei, [2]Chen Xuedan, [2]Yan Shiting, [2]Zhang Zhengliang, [2]Chen Yuqin, [2]Zheng Lina
[2]Zhu Guangqi and [2]Han Xiaoxiang*
[1]*Jiangsu Key Laboratory of Regional Resource Exploitation and Medicinal Research, Huaiyin Institute of Technology, Huaian 223003, P. R. China.*
[2]*Department of Applied Chemistry, Zhejiang Gongshang University, Hangzhou 310018, P. R. China*.
hxx74@126.com*

(Received on 18th April 2019, accepted in revised form 24th August 2020)

Summary: A series of silica gel (SG) supported metal ionic liquid catalysts (*x*[Bmim]Cl-$CrCl_3$/SG) were synthesized and exploited for the esterification of palmitic acid (PA) with methanol (ML) to produce biodiesel efficiently. The 10%[Bmim]Cl-$CrCl_3$/SG catalyst with high surface area and desirable acidity exhibited the best catalytic performance and reusability after six consecutive running cycles. Based on the response surface analysis, the optimal reaction conditions were obtained as follows: methanol/acid mole ratio = 11:1 mol/mol, catalyst amount = 5.3 wt%, reaction time = 65 min, as well as reaction temperature = 373 K, reaching to a biodiesel yield of 96.1%. Further kinetic studies demonstrated that the esterification of PA with ML obeyed 1.41 order kinetics for acid concentration with the activation energy of 16.88 kJ/mol.

Keywords: Esterification, Ionic liquid, Silica gel, Biodiesel, Response surface methodology.

Introduction

Biodiesel, an eco-friendly potential renewable energy, can effectively reduce emissions of pollutants and greenhouse gases, and it can also serve as an ideal substitute for petrochemical diesel [1]. Nowadays, with the rising price of crude oil and the increasing number of environmental problems, more researchers are attracted to the biodiesel production [2]. The catalytic preparation of biodiesel normally includes transesterification and esterification [3, 4]. Ordinarily, biodiesel, namely fatty acid alkyl esters, is commonly synthesized by transesterification with strong basic catalysts (including homogeneous and heterogeneous catalysts), which has contributed to undesirable side reactions and resulted in a large accumulation of glycerol in the by-products, as well as long reaction time and high energy consumption [5, 6]. Currently, considerable attention has been paid to biodiesel prepared by esterification with long chain free fatty acids and lower alcohols as raw materials [7].

Biodiesel is often made up of alkyl esters, and it normally consists of methyl (ethyl) esters of the fatty acids from the fat or parent oil [8]. Widely found in oils, fats, milk and cheeses, palmitic acid is regarded as one of the most common saturated fatty acids and it presents in both edible oils and non-edible oils with an amount of about 4-23%. Methyl palmitate, prepared by esterification of palmitic acid and methanol, can be used not only as an intermediate for the preparation of fine chemicals including emulsifiers, wetting agents, stabilizers, etc, but also as an important biodiesel [9, 10]. Traditionally, the production of methyl palmitate is normally synthesized by esterification using acidic catalysts such as H_2SO_4, H_3PO_4 or *p*-toluene sulfonic acid. It is undeniable that these catalysts have disadvantages of severe corrosiveness, undesirable environmental pollution and formidable separation, which have limited their large-scale industrialization [11]. In addition, heteropoly acids [12], super solid acid [13], zeolites [14], metallic oxide [15], and other catalysts are also introduced in the esterification reaction. However, these solid catalysts are limited in application on account of their defects such as easy deactivation, low activity, being difficult to separate and recycle, and so on [16]. Accordingly, the development of environmentally friendly catalysts is of great importance to solve the above problems.

Recently, ionic liquid has drawn much attention as a green catalyst and solvent. What's more, ionic liquid has been extensively employed for alkylation, oxidation, hydration/dehydration, as well as transesterification and esterification [17, 18], especially in the preparation of biodiesel [19, 20]. However, ionic

*To whom all correspondence should be addressed.

liquids are expensive and difficult to separate in reaction systems, thus limiting the large-scale use of ionic liquids to some extent. Luckily, problems above can be effectively solved by using silica [21], SBA-15 [22], rod-like carbon [23] and other porous materials to immobilize ionic liquids.

In this work, silica gel-supported metal ionic liquid (MIL/SG) catalysts have been prepared and exploited for catalytic synthesis of methyl palmitate. These MIL/SG catalysts were characterized by Fourier-transform infrared (FT-IR), thermogravimetric analysis (TGA) and Raman spectroscopy. The MIL/SGs possess unique characteristics, which is favorable for catalyst separation, recovery, and good catalytic activity with reduced usage of expansive ionic liquids. Furthermore, the effects of major reaction variables were investigated and the kinetics of the esterification reaction was evaluated under the optimized conditions by means of response surface methodology (RSM) [24, 25].

Experimental

Catalyst preparation

Silica gel supported metal ionic liquid catalysts (*x*%[Bmim]Cl-$CrCl_3$/SG) were synthesized in the laboratory according to the process outlined in the literature [26,27]. At the beginning of the procedure, N-methyl imidazole (0.2 mol), *n*-butyl chloride (0.28 mol) and desirable acetonitrile were stirred at reflux temperature (358 K) for 48 h. Upon completion, the mixture was distilled off by rotary evaporation, washed five times with acetonitrile and ethyl acetate (volume ratio 1:5), and then dried under vacuum. Afterwards, the stoichiometric amount of $CrCl_3 \cdot 6H_2O$ (0.2 mol) was added into the precursor ionic liquid 1-butyl-3-methyl-imidazolium chloride. Under nitrogen atmosphere, the mixture was continuously stirred for 24 h at 303 K. The metal ionic liquid was obtained and abbreviated as [Bmim]Cl-$CrCl_3$. By the sol-gel method, the silica gel supported metal ionic liquid catalyst was successfully prepared [27]. A certain amount of metal ionic liquid [Bmim]Cl-$CrCl_3$, ethanol and tetraethyl orthosilicate (TEOS) were mixed under stirring condition, and then the mixture was acidified with HCl. After the reaction for 18 h at 333 K, the obtained mixture was aged for 12 h under room temperature, and then calcined at 473 K for 5 h to obtain the silica gel supported metal ionic liquid catalysts. The catalysts were defined as *x*%[Bmim]Cl-$CrCl_3$/SG, where *x* represents the mole contents of [Bmim]Cl-$CrCl_3$ (*x* = 5, 10, 20 and 30).

Catalyst characterization

The chemical bond vibration in the structure of the catalysts was first characterized by FT-IR. On the Bruker Vertex 70 FT-IR instrument, the sample was prepared by KBr pellet method, and the infrared spectrum of the catalysts was observed over the wavenumber range of 4000~400 cm^{-1}. Stability of the catalyst was characterized by thermogravimetric and differential thermogravimetric (TG-DTG). Under N_2 protection condition, the sample was tested at a range from 313 K to 873 K with the rate of 10 K/min. The structural properties of the various catalysts were also investigated by N_2 adsorption/desorption isotherms with a physisorption apparatus (Micromeritics, ASAP 2020). All Raman spectra were recorded by RM1000 laser confocal microscopy Raman spectrometer from British Renishaw company with laser wavelength of 514 nm over the range of 1000~200 cm^{-1}.

Esterification reaction

The typical esterification procedure was: a desirable number of palmitic acid, methanol and *x*%[Bmim]Cl-$CrCl_3$/SG (*x* = 5, 10, 20 and 30) were added into a 100 mL three-necked flask. The flask was connected with a reflux condenser, a mechanical stirrer, and a dropping funnel including 3 Å molecular sieves to separate part of the water produced from the reaction. The reaction mixture was stirred at 373 K for a certain time. After reaction, the mixture was cooled down to room temperature. The catalyst was separated and washed with ethyl acetate to be reused. The sample was analyzed by a gas chromatographer (Agilent 7890B) equipped with a HP-5 capillary column and a flame-ionization detector (FID) using methyl laurate as an internal standard. The way to calculating palmitic acid conversion and biodiesel yield was consistent with our previous research [12].

Response surface methodology

Based on the single factor method, 17 groups of experiments were designed by RSM to optimize the preparation conditions of methyl palmitate during esterificaton of PA with ML over the 10%[Bmim]Cl-$CrCl_3$/SG catalysts. In the process of biodiesel production, the relationship among three key variables (ML/PA mole ratio(x_1), amount of catalyst(x_2), reaction time(x_3)) was analyzed. As shown in Table-1, each variable was coded at three levels: low level (−1), central value (0), high level (+1). The influence of the variables on methyl palmitate yield (*Y*) was also investigated. According to the Design-Expert 8.0.7.1

(Stat-Ease, USA) software, the design of experiments and analyses of experimental data were obtained, with the coded values of these factors shown by eqn(1) [24]:

$$x_i = \frac{X_i - X_0}{\Delta X_i} \quad (1)$$

where X_0, x_i and X_i, (i = 1-3) meant the central, coded, and real value of the various variables, respectively, and ΔX_i represented the step-change value. Utilizing the quadratic polynomial model equation given by RSM, the interactive effects between experimental variables were studied to make the reaction process as effective as possible and predict the yield of methyl palmitate. The second-order equation model can be shown as:

$$Y = \beta_0 + \sum_{i=1}^{3} \beta_i x_i + \sum_{i=1}^{3} \beta_{ii} x_i^2 + \sum_{i<j}^{3} \beta_{ij} x_i x_j \quad (2)$$

where Y represented the predicted yield of methyl palmitate, x_i and x_j were the levels of code for independent variables. β_0, β_i, β_{ii}, as well as β_{ij} denoted the regression coefficient of the offset, linear, quadratic, and interactive term for the variables, respectively.

Table-1: Coded values and parameter levels used in the experimental design.

Variable (unit)	Symbol	Level and range		
		–1	0	+1
ML/PA mole ratio (mol/mol)	x_1	8	10	12
Amount of catalyst (wt%)	x_2	4	5	6
Reaction time (min)	x_3	45	60	75

Kinetic study

The esterification of PA and ML is a reversible reaction. Under experimental conditions, the main product is methyl palmitate when the biodiesel is prepared with PA and ML as raw materials. The rate equation can be indicated as:

$$r = -\frac{dC_A}{dt} = k_+ C_A^{\alpha} C_B^{\beta} - k_- C_C^{\gamma} C_D^{\eta} \quad (3)$$

where r was reaction rate, k_+ and k_- represented the forward and reverse rate constants, respectively. C_A, C_B, C_C, and C_D indicated the concentration of PA, ML, methyl palmitate, and H_2O, respectively. α, β, γ, and η donated the reaction order for above variables.

In the reaction, the methanol concentration was much higher than palmitic acid. The water produced in the reaction was carried away by 3Å molecular sieves in the constant pressure funnel. Therefore, the reaction can be regarded as irreversible reaction, and C_B^{β} in eqn (3) could be considered as constant, so the $k_+ C_B^{\beta}$ can be deemed as the modified rate constant (k), the eqn(3) can be simplified as eqn(4):

$$r = -\frac{dC_A}{dt} = kC_A^{\alpha} \quad (4)$$

Taking the natural logarithm of eqn(4), the above equation can be expressed as eqn(5):

$$\ln r = \ln k + \alpha \ln C_A \quad (5)$$

By drawing the curve of C_A with time (t), and linear fitting of the ln r and ln C_A curve, the k value and the reaction order at different temperatures can be obtained. Moreover, the Arrhenius equation which donated the relationship between the rate constant and temperature can be shown as:

$$\ln k = \ln k_0 - \frac{E_a}{R}\frac{1}{T} \quad (6)$$

where E_a was the activation energy during esterification of PA and ML over the 10%[Bmim]Cl-$CrCl_3$/SG catalyst, k_0 represented the pre-exponential factor, R was the gas constant, and T denoted reaction temperature.

Results and Discussion

Catalyst characterization

FT-IR spectra of silica gel supported metal ionic liquid catalysts (x%[Bmim]Cl-$CrCl_3$/SG, x = 5, 10, 20, and 30) were compared in Fig. 1, which elucidated the chemical composition and configuration of the various catalysts. The FT-IR spectra of [Bmim]Cl-$CrCl_3$ catalyst was similar to [Bmim]Cl (Fig. 1a, Fig. 1b and Fig. 2). In the spectra of ionic liquids [Bmim]Cl-$CrCl_3$, the absorption peaks at 3420 cm^{-1} represented the stretching vibrations of C-H on the imidazole ring [28]. The peaks at 2952 and 2850 cm^{-1} may be caused by the stretching vibrations of -CH and -CH_2 on the alkyl chain. The bands at approximately 1640 and 1562 cm^{-1} were ascribed to the stretching vibrations of C=C and C=N bands on the imidazole ring, while the bands at 1464 and 1167 cm^{-1} corresponded to the bending vibrations of C-N on imidazole ring and C-N on butyl side chain. In particular, the absorption peak at 750 cm^{-1} indicated bending vibrations of -CH_3. The peak at 626 cm^{-1} may arise from the stretching vibrations of C-Cl [28]. Upon anchoring the metal ionic liquid onto the silica gel

support, MIL/SG catalysts showed not only the anticipated features of the [Bmim]Cl-$CrCl_3$ (Fig. 1b and Fig. 2b) but also characteristic absorption bands arising from the SG support (Fig. 1c), as illustrated in Fig. 1d–h. The absorption peaks at 3432 cm^{-1} represented the stretching vibrations of hydroxyls (-OH) functional group [29]. What's more, the absorption bands near 943 and 805 cm^{-1} were owing to symmetric stretching vibration of Si(OC_2H_5) and symmetric stretching vibration of Si-O-Si [30]. Overall, the above results clearly indicated that the MIL, namely [Bmim]Cl-$CrCl_3$, was successfully immobilized on the SG support.

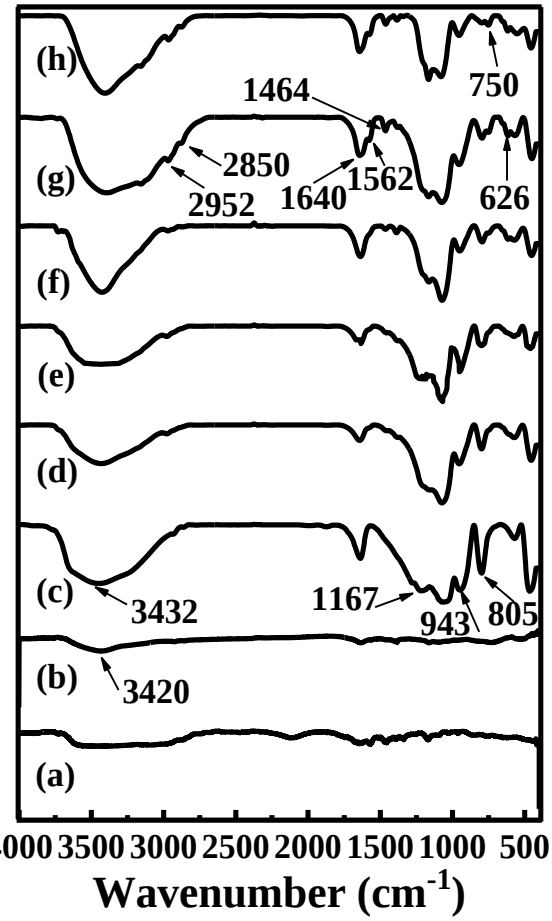

Fig. 1: FT-IR spectra of (a) [Bmim]Cl, (b) [Bmim]Cl-$CrCl_3$, (c) bare SG, and various supported *x*%[Bmim]Cl-$CrCl_3$/SG catalysts with different [Bmim]Cl-$CrCl_3$ loadings, *x*, of (d) 5 %, (e) 10 % (fresh), (f) 10 % (spent), (g) 20 %, and (h) 30 %.

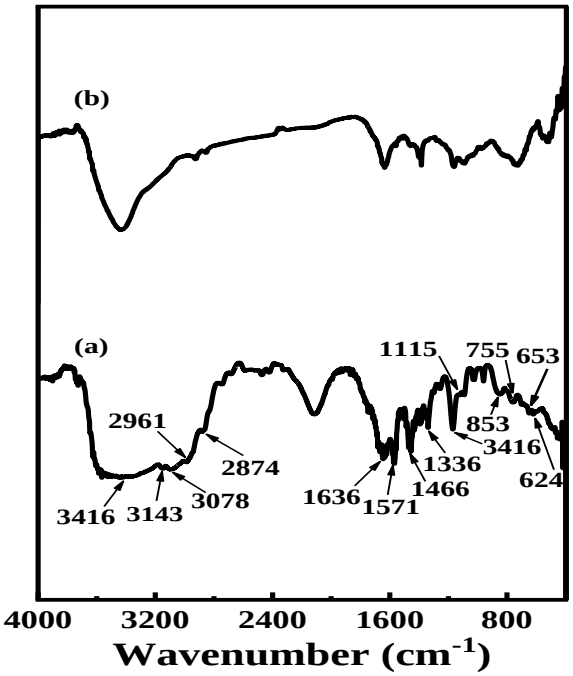

Fig. 2: FT-IR spectra of (a) [Bmim]Cl, (b) [Bmim]Cl-$CrCl_3$.

With the help of TG-DTG technique, the thermal properties and structural stabilities of various catalysts were further investigated. Since similar TG-DTG profile was shown by all MIL/SG samples over the temperature range of 303-873 K, only the curve for the 10%[Bmim]Cl-$CrCl_3$/SG sample was illustrated and discussed. The thermal stability of precursor of ionic liquid [BMIM]Cl was shown in Fig. 3a. An initial weight loss occurring at ca. 404 K may be due to desorption of physisorbed water. The second peak of weight loss at ca. 556 K may be ascribed to the disassembly of the organic fraction. As shown in Fig. 3b, the curves of [Bmim]Cl-$CrCl_3$ showed two main weight-loss peaks. The first weight loss at ca. 420 K was due to the elimination of water adsorbed on the surface. The second weight loss over the temperature range of 550-750 K was reasonable due to the decomposition of ionic liquid and precursor of ionic liquid [BMIM]Cl. Likewise, the TG-DTG profile of the 10%[Bmim]Cl-$CrCl_3$/SG catalyst in Fig. 3c also showed two main weight-loss peaks at ca. 340 and 630 K, which may arise from the detachment of physisorbed water and decomposition of organic components in the supported catalyst. The thermal analysis results also indicated that the metal ionic liquid [Bmim]Cl-$CrCl_3$ was successfully immobilized on the SG support and was stable under the temperature used in the experiment.

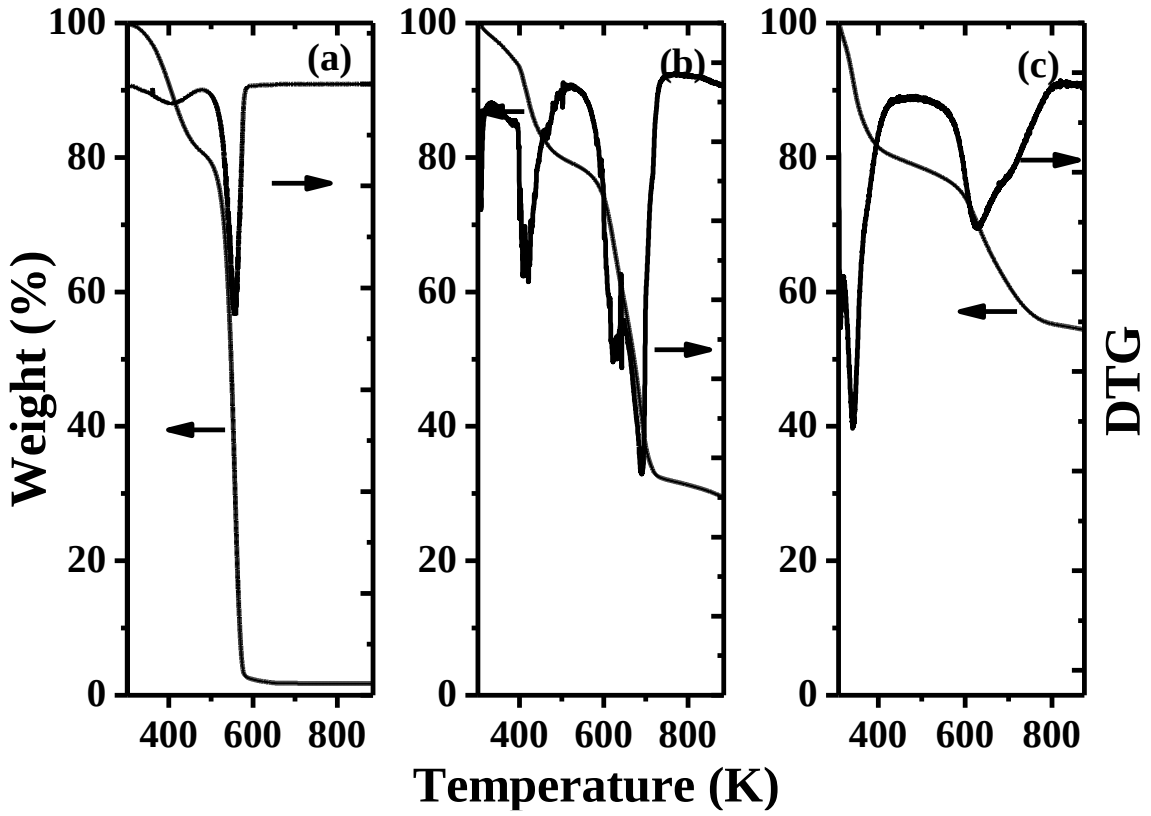

Fig. 3: TG-DTG profiles of (a) [Bmim]Cl, (b) [Bmim]Cl-$CrCl_3$ and (c) 10%[Bmim]Cl-$CrCl_3$/SG.

Additional N_2 physisorption study (not shown) further revealed that the textural properties of the supported catalyst had an important impact on catalytic activity during the esterification reaction. The bare SG support exhibited high surface areas (536 m^2/g), and the addition of [Bmim]Cl-$CrCl_3$ seemed to have a large impact on the surface area. Superficial areas of 375, 201, 53.2, and 5.8 m^2/g were derived for 5%[Bmim]Cl-$CrCl_3$/SG, 10%[Bmim]Cl-$CrCl_3$/SG, 20%[Bmim]Cl-$CrCl_3$/SG, and 30%[Bmim]Cl-$CrCl_3$/SG catalyst, respectively. The results indicated a progressive anchoring of the metal ionic liquid in pore channels of the silica gel support.

Raman spectra of silica gel supported metal ionic liquid catalysts (*x*%[Bmim]Cl-$CrCl_3$/SG, *x*=5%, 10%, 20%, 30%) were taken to further prove the presence of various loading catalysts, and the results were exhibited in Fig. 4. As revealed in Fig. 4, all the catalysts had broad absorption peaks over the 500-300 cm^{-1} region which were attributed to [Bmim]Cl-$CrCl_3$. Among various supported metal ionic liquid catalysts, with increasing dosage of ionic liquid [Bmim]Cl-$CrCl_3$, the intensity of absorption peak was increasing. The results indicated that various supported catalysts kept the completeness of the ionic liquid structure.

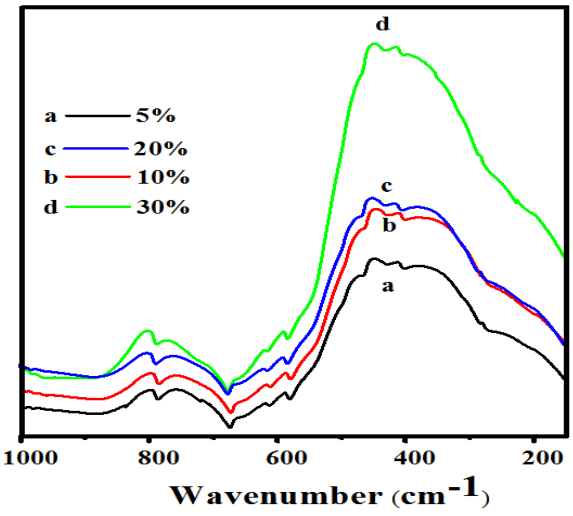

Fig. 4: The Raman spectra of various supported *x*%[Bmim]Cl-$CrCl_3$/SG catalysts with different [Bmim]Cl-$CrCl_3$ loadings, *x*, of (a) 5%, (c) 10 %, (d) 20 %, and (e) 30 %.

Role of x%[Bmim]Cl-$CrCl_3$/SG on catalytic activity

To assess the catalytic activity of multifarious catalysts during the esterification, the performances of silica gel, Lewis ionic liquid, and MIL/SG catalysts were compared. The results were summarized in Table-2. The data depicted in Table-2 were average values from three parallel entries. The catalytic activity of [Bmim]Cl-$CrCl_3$ and silica gel was inferior compared with *x*%[Bmim]Cl-$CrCl_3$/SG. Among various supported metal ionic liquid catalysts, 10%[Bmim]Cl-$CrCl_3$/SG catalyst exhibited superior catalytic performance. The palmitic acid conversion and biodiesel yield were 94.9% and 94.4%, respectively. The esterification reaction is a representative acid-catalyzed reaction. With the loading of the metal ionic liquid increasing, the Lewis acidic property of sample was strengthened, leading to the enhancement of catalytic activity. However, the excessive acidity was not conducive to the esterification reaction. Meanwhile, the specific surface area of the SG support indeed also showed an important impact on the esterification reaction. As the loading of metal ionic liquid increasing, the surface area of the catalyst reduced greatly. High catalytic properties were ascribed to the desirable acidity and the high surface area of catalyst. Immobilizing MIL on SG supports not only avoided the difficulty to separate the catalyst from reaction system caused by the high viscosity of the ionic liquid, but also greatly reduced the use amount of the ionic liquid and lowered the overall cost while maintaining high catalytic activity [31]. Accordingly, 10%[Bmim]Cl-$CrCl_3$/SG catalyst was adopted for process optimization and kinetic studies during the esterification of ML and PA (*vide infra*).

Table-2: Catalytic performance of PA esterification with ML over *x*[Bmim]Cl-$CrCl_3$/SG catalysts[a].

Catalyst	Conversion (%)[b]	Yield (%)[c]
Silica gel	**31.8**	**31.4**
[Bmim]Cl-$CrCl_3$	**41.3**	**40.6**
5%[Bmim]Cl-$CrCl_3$/SG	**61.2**	**60.7**
10%[Bmim]Cl-$CrCl_3$/SG	**94.9**	**94.4**
20%[Bmim]Cl-$CrCl_3$/SG	**86.1**	**85.8**
30%[Bmim]Cl-$CrCl_3$/SG	**83.7**	**83.2**

[a]Reaction conditions: 373 K, ML/PA = 10:1 (mole ratio); 5wt% catalyst amount relative to PA, 60 min. [b]Conversion of PA was based on acid number. [c]GC yield.

Effects of reaction parameters on esterification

The effects of mole ratio of reactants, amount of catalyst, reaction time and reaction temperature on the esterification of PA with ML were further studied using 10%[Bmim]Cl-$CrCl_3$/SG as catalyst. The experiments were carried out by changing one variable while keeping other variables constant, and the results were listed in Fig. 5. The impact of ML/PA molar ratio on the preparation of methyl palmitate was displayed in Fig. 5a, which could be seen that the methyl palmitate yield increased with increasing ML/PA mole ratio. The highest yield of biodiesel obtained was 94.4% with ML/PA molar ratio of 10:1 in 60 min. The excess of methanol provided more opportunity for collisions of reactant molecules and then shifted the equilibrium to biodiesel. However, the yield of biodiesel decreased with the increasing of ML/PA molar ratio, which may be due to the over dilution of PA and catalyst, and the concentration of active acid center decreased with excessive methanol. This was in line with the previously reported literature [12]. Thus, an optimal ML/PA molar ratio of 10:1 was chosen for the esterification.

The effect on the conversion of PA by the catalyst amount was displayed in Fig. 5b. The yield of biodiesel improved almost linearly with the catalyst amount up to *ca*. 5 wt% and achieved a maximum of biodiesel (94.4%) when the catalyst amount was 5 wt% within 60 min. The reason was that not enough active fractions could be applied for the esterfication with low catalyst amount. The amount of active acid sites available increased significantly with catalyst amount increasing. Nevertheless, further increasing catalyst amount, the biodiesel yield was gradually decreased. An excessive catalyst amount tended to cause formation of undesirable by-products. The detail evidences have yet to be investigated. Considering the product yield and less cost efficiency, the optimal amount of 10%[Bmim]Cl-$CrCl_3$/SG should be kept at about 5 wt%.

Changing the reaction time by 15 to 90 min with the conditions of ML/PA mole ratio = 10:1, catalyst amount = 5 wt%, and reaction temperature = 373 K, the effect of reaction time on biodiesel yield was studied and the results were listed in Fig. 5c. According to Fig. 5c, the yield of biodiesel increased from 70.3% to 94.4% with reaction time increasing from 15 to 60 min. The yield of biodiesel declined slightly with further increasing reaction time. This may be ascribed to that the by-products of reaction emerged and increased at prolonged reaction time (> 60 min). Therefore, 60 min was selected as optimum reaction time for further study.

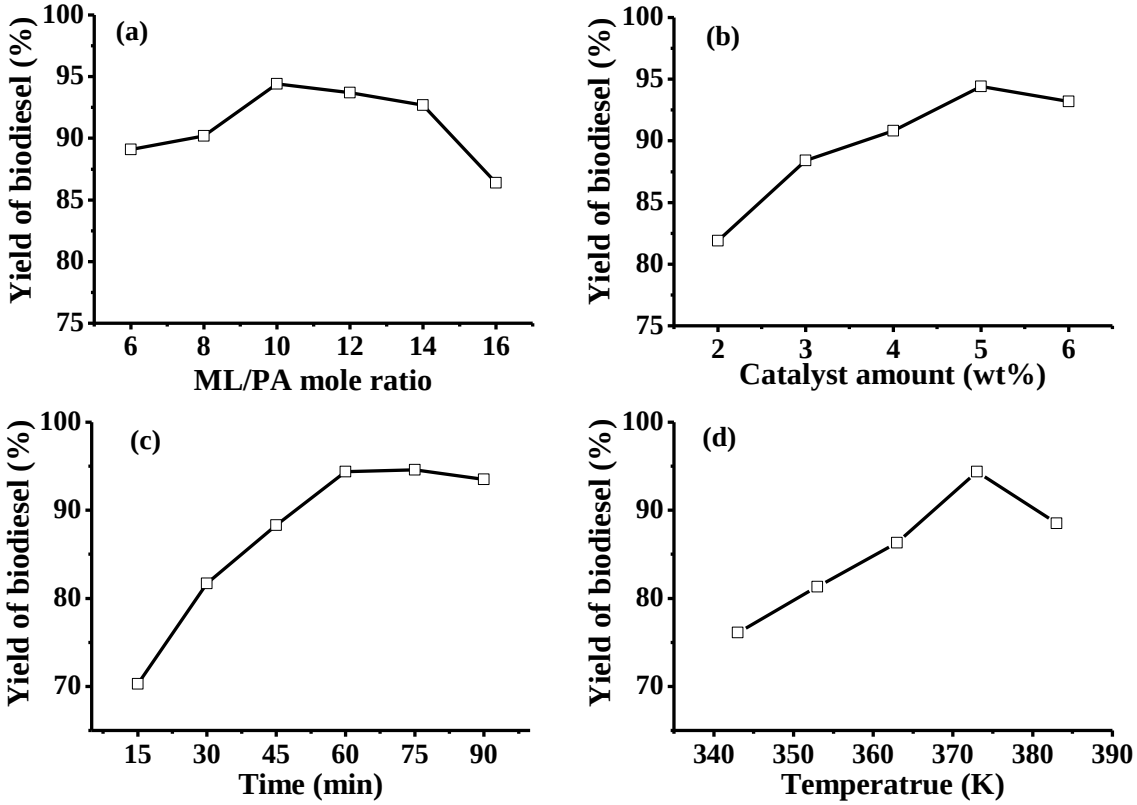

Fig. 5: Effects of four factors on the yield of biodiesel during esterification of PA with ML over 10%[Bmim]Cl-$CrCl_3$/SG catalyst: (a) ML/PA molar ratio, (b) catalyst amount, (c) time and (d) temperature.

Fig. 5d displayed the influence of temperature (over the range of 343-383 K) on biodiesel yield while other reaction parameters were kept fixed. It was also found that the catalytic activity initially enhanced with temperature increasing and the highest yield of biodiesel was obtained with 94.4% at 373 K in 60 min. The yield of biodiesel was much higher than that of yield (85.5%) obtained without water removal. Further increasing the temperature, the biodiesel yield descended rapidly. As expected, the reaction rate was slower at lower temperatures, but adverse side effects may occur at higher temperature so that the selectivity of the target product was reduced [32,33]. Thus, the optimum temperature of 373 K was used in the experiment.

In summary, an optimum catalytic activity related to biodiesel yield (94.4%) was obtained over the 10%[Bmim]Cl-$CrCl_3$/SG catalyst with ML/PA = 10:1, catalyst amount = 5 wt%, time = 60 min, and temperature = 373 K, as shown in Fig. 5, respectively. The result was higher than those obtained under optimal conditions for the similar reaction over the SBA-15 supported 1-(3-sulfonate)-propyl-3-allylimidazolium dihydrogen phosphotungstate (SIL-3) (88.1%) [34], sulfated zirconia (SZr) (90%) [35], $[MIM\text{-}PSH]_{2.0}HPW_{12}O_{40}$ (91.8%) [11], and $[GlyH]_{1.0}H_{2.0}PW_{12}O_{40}$ (93.3%) [12].

Process and product optimization

The optimization of synthesis process of methyl palmitate, which based on response surface methodology (RSM), can improve the yield of methyl palmitate and avoid the tedious experiments. 17 groups of experimental conditions and results were listed in Table-3. The yield of biodiesel (Y) related to independent experimental variables using multiple regression analysis can be expressed as the quadratic model:

$$Y = 94.41 + 2.70x_1 - 2.97x_2 + 2.28x_3 - 2.09x_1^2 - 4.71x_2^2 - 3.19x_3^2 - 1.89x_1x_2 - 0.95x_1x_3 + 0.88x_2x_3 \quad (7)$$

Table-3: Box-Behnken design (BBD) and response values.

Run	Variable and value			Biodiesel yield (%)	
	x_1	x_2	x_3	Experimental	Predicted
1	8	4	60	80.08	80.04
2	12	4	60	89.85	89.21
3	8	6	60	89.12	89.76
4	12	6	60	91.35	91.39
5	8	5	45	83.17	83.19
6	12	5	45	89.88	90.50
7	8	5	75	90.27	89.65
8	12	5	75	93.16	93.14
9	10	4	45	82.12	82.14
10	10	6	45	86.97	86.31
11	10	4	75	84.27	84.92
12	10	6	75	92.65	92.63
13	10	5	60	94.31	94.41
14	10	5	60	94.09	94.41
15	10	5	60	94.43	94.41
16	10	5	60	95.53	94.41
17	10	5	60	93.67	94.41

The positive sign in the first and two terms indicated the synergy between the specified variables, and the negative sign represented the antagonism. The fitting quality of quadratic model (eqn (7)) was validated by the standard analysis of variance (ANOVA), as listed in Table-4.

Table-4: ANOVA data for the prediction of Methyl palmitate yield by the proposed quadratic model.

Source	Sum of squares	DF[a]	Mean square	*F*-value	*Prob* > *F*	Significant[b]
Model	361.99	9	40.22	64.69	< 0.0001	**
x_1	58.32	1	58.32	93.80	< 0.0001	**
x_2	70.63	1	70.63	113.60	< 0.0001	**
x_3	41.45	1	41.45	66.67	< 0.0001	**
x_1^2	18.47	1	18.47	29.70	0.0010	**
x_2^2	93.48	1	93.48	150.35	< 0.0001	**
x_3^2	42.89	1	42.89	68.99	< 0.0001	**
x_1x_2	14.21	1	14.21	22.86	0.0020	**
x_1x_3	3.65	1	3.65	5.87	0.0459	*
x_2x_3	3.12	1	3.12	5.01	0.0602	
Residual	4.35	7	0.62			
Lack of Fit	2.44	3	0.81	1.70	0.3043	NS
Pure Error	1.91	4	0.48			
Cor Total	366.34	16				

[a] DF denotes degree of freedom.

[b]* Represents significant; ** represents highly significant; NS = not significant.

The significance of variables can be evaluated by *P*-value in Table-4. The model *F*-value of 64.69 was much greater than the corresponding counterpart in the Table ($F_{0.01, 9, 7} = 6.71$), and the *P*-value was lower than 0.0001, meaning that the model was indeed significant. The *F*-value of "the Lack of fit" was 1.70, which showed that the Lack of Fit was not significant corresponding to pure error. The "Adeq Precision" was 23.75, which was also much higher than the ideal value of 4. Moreover, the "Pred *R*-Squared" of 0.9881 was in line with the "Adj *R*-Squared" of 0.9728 reasonably. The *P*-values of x_1, x_2, x_3, x_1^2, x_2^2 and x_3^2 were less than 0.01, indicating that the three variables were highly significant. In addition, the *P*-value of cross terms x_1x_2 was less than 0.01, representing that the experimental factors showed highly significant interaction between ML/PA molar ratio and the amount of catalyst. The *P*-value of cross terms x_1x_3 was less than 0.05, showing that there was significant interaction between ML/PA molar ratio and reaction time.

The relationship between several experimental variables can be explained by the response surface and contour plots in Fig. 6. The shape and density of contour plots can reflect the interaction on the yield of biodiesel between different variables while keeping the other variable at a central value. The elliptical contour indicated that the reciprocity between the two variables had a significant impact on the yield of biodiesel. A denser contour curve showed a greater effect on the biodiesel yield.

As shown in Fig. 6(a,d), the correlation between ML/PA molar ratio (x_1) and catalyst amount (x_2) and the effect on response value were highly significant, judged by elliptical contour shape. And the conclusion was in accord with the ANOVA data in Table-4. Moreover, the contour lines along x_2 direction were more intensive, indicating that x_1 had a more significant impact on biodiesel yield than x_2 under fixed reaction temperature and time. Likewise, the impact of x_1 and x_3 on response value can be inferred from Fig. 6(b,e). The effects of x_1 and x_3 on the yield of biodiesel were similar, and the interaction of x_1 and x_3 was significant. Furthermore, the circle contour shape (Fig. 6(c,f)) observed for catalyst amount (x_2) with reaction temperature (x_3) meant that the interaction between them was insignificant, which was in excellent agreement with the ANOVA data.

According to the above response surface analysis results, the predicted yield of biodiesel obtained by esterification of ML with PA over 10%[Bmim]Cl-$CrCl_3$/SG catalyst was 96.46% under the optimized reaction conditions: x_1 (ML/PA molar ratio) = 11.12 mol/mol, x_2 (catalyst amount) = 5.33 wt%, x_3 (reaction time) = 65.4 min, and reaction temperature = 373 K. To demonstrate the availability of the model and optimum process conditions, three sets of parallel experiments were performed at 373 K with x_1 = 11:1, x_2 = 5.3 wt%, x_3 = 65 min, and the average yield of biodiesel was 96.1%. The results were in agreement with predicted yield, indicating that the proposed model was accurate.

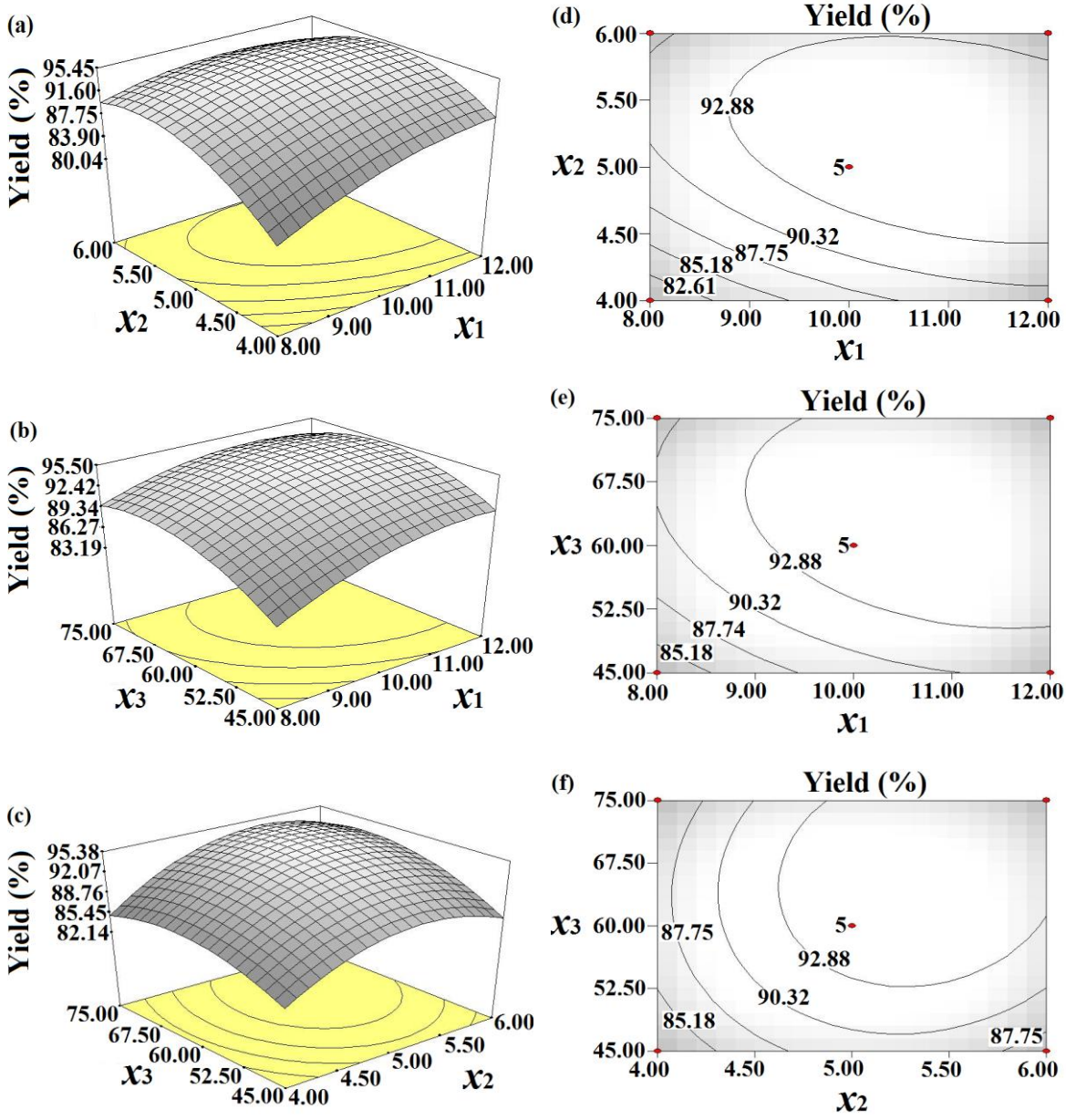

Fig. 6: Response surface (a–c) and contour plots (d–f) showing the predicted values of methyl palmitate yield, (a) and (d) ML/ PA molar ratio vs. catalyst amount, (b) and (e) ML/ PA molar ratio vs. reaction time, (c) and (f) catalyst amount vs. reaction time. Other variables are held at constant level.

Catalyst recycling

The stability and utilization of the catalyst have a significant effect on reducing the cost of the experiment. What's more, the feasibility of catalyst separation from reaction system is prominent characteristic of supported catalyst. As an illustration, the stability of the 10%[Bmim]Cl-$CrCl_3$/SG catalyst was investigated under the above optimal operation conditions. After each reaction, the catalyst was filtered from the reaction system. Then the spent catalyst was washed by acetic ether, followed by drying under vacuum at 353 K for 8 h before reused. The results were listed in Fig. 7. From Fig. 7, we found that the 10%[Bmim]Cl-$CrCl_3$/SG catalyst exhibited good stability. The yield of biodiesel decreased from 96.1% of the first run to 86.9% after six continuous running cycles. The spent catalyst (Fig.

1f) retained all characteristic bands of the fresh 10% [Bmim]Cl-$CrCl_3$/SG catalyst (Fig. 1e) except for slight decrease in their peak intensities. According to elemental analyses of ICP, the concentration of N atom was reduced from 3.1 wt% of the fresh catalyst to 2.7 wt% in the regenerative spent catalyst. In addition, the specific surface area of the 10%[Bmim]Cl-$CrCl_3$/SG catalyst also decreased from 201 to 176 m^2/g after six consecutive runs. These above results indicated that the decrease of catalytic activity may be ascribed to the loss of [Bmim]Cl-$CrCl_3$ during recovery and regeneration processes. The results also confirmed the stability and recyclability of the silica gel supported metal ionic liquid catalysts.

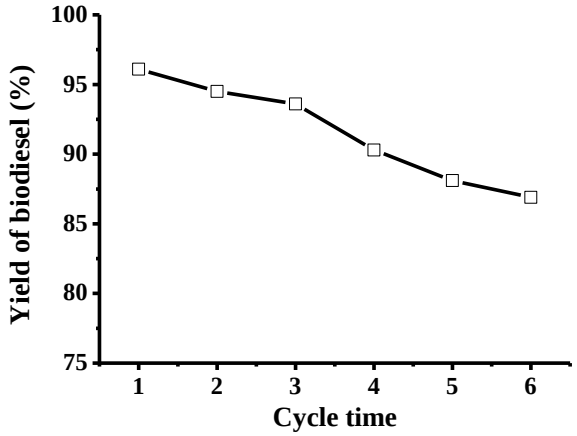

Fig. 7: The recycle results of the PA esterification catalyzed by 10%[Bmim]Cl-$CrCl_3$/SG.

Kinetic modeling

In order to establish a kinetic model for the synthesis of biodiesel (methyl palmitate) over 10%[Bmim]Cl-$CrCl_3$/SG catalyst under the above optimized conditions, the experiments were carried out at temperatures of 333, 343, 353, 363 and 373K, respectively. Other conditions were conducted with catalyst amount of 5.3 wt% and ML/PA molar ratio of 11:1 mol/mol, and the reactions were analyzed at a reaction time of 10, 20, 30 and 45 min at each temperature, respectively. The change of PA concentration with time at different temperatures was shown in Fig. 8. Using Origin 8 software, the instant reaction rate (r) of different moments at different temperatures was obtained from the curve integral. According to equation (5), the reaction values of α and k under different temperatures can be acquired in Fig. 9a. Taking the experiment conducted at 333 K as an instance, the relationship diagram of ln r versus ln C_A fitted eqn(5) well with a correlation coefficient (R) of 0.9652. What's more, Table-5 showed the values of α and k under different temperatures. Therefore, the average reaction order α of methyl palmitate prepared by esterification reaction was 1.41. Based on eqn(6), the pre-exponential factor k_0 = 17.12 and reaction activation energy E_a = 16.88 kJ·mol^{-1} may also be derived from the intercept and slope of the Arrhenius plot listed in Fig. 9b. Consequently, the kinetic equation of the esterification reaction under the optimal conditions may be expressed as:

$$r = -\frac{dC_A}{dt} = 17.12\, exp\left(-\frac{16.88}{RT}\right) C_A^{\,1.41}.$$

Table-5: List of α and ln$k$ within certain temperature ranges during the esterification of PA and ML over the10%[Bmim]Cl-$CrCl_3$/SG catalyst.

Temperature/K	ln k	α
333	-3.07	1.23
343	-2.83	1.46
353	--2.69	1.38
363	-2.56	1.43
373	-2.42	1.53

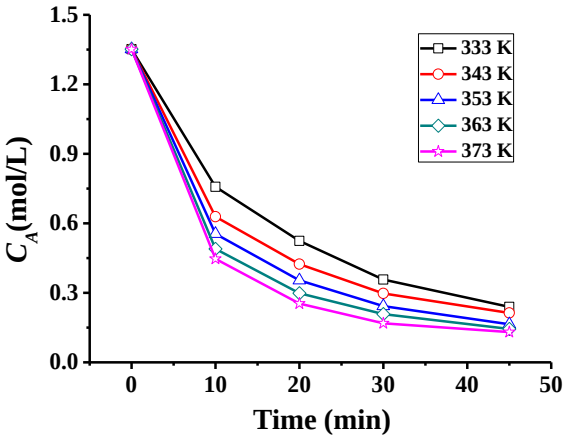

Fig. 8: Instantaneous concentration of PA (C_A) with reaction time within certain temperature ranges.

It is remarkable that the E_a value of esterification process of PA and ML over 10%[Bmim]Cl-$CrCl_3$/SG catalyst is much smaller compared to that observed for esterification of PA and deuterated ML over p-sulfonic acid calix [4] arene catalyst (22.0 kJ/mol^{-1}) [36] and the esterification of free fatty acids and methanol over niobium oxide supported 12-tungstophosphoric acid (25%TPA/Nb_2O_5) catalyst (57.18 kJ/mol^{-1}) [37]. The above results indicated that the 10%[Bmim]Cl-$CrCl_3$/SG catalyst was an efficient catalyst with high activity for esterification of PA to biodiesel.

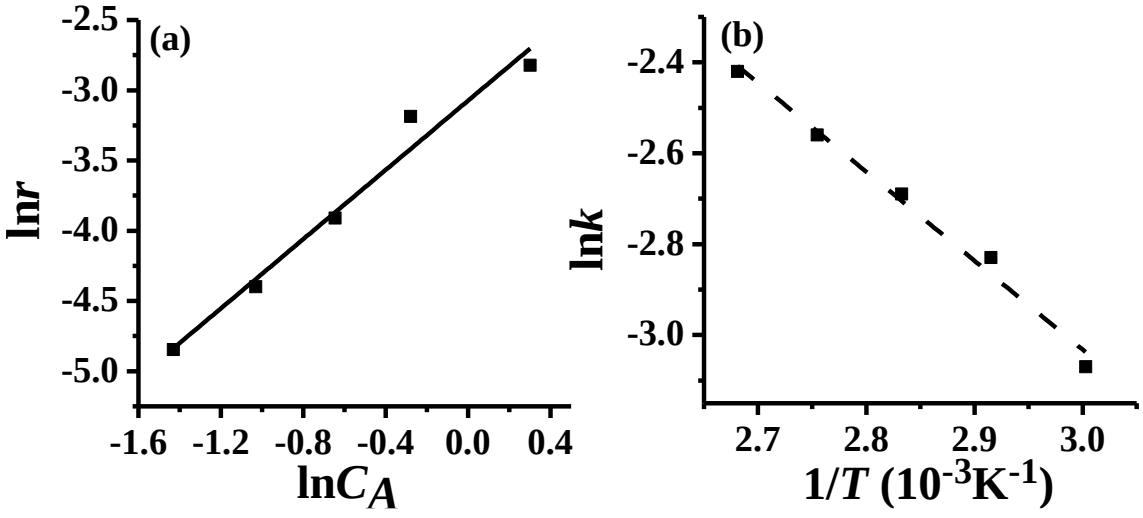

Fig. 9: (a) Plot of ln*r* *vs* lnC_A at 333 K, and (b) Arrhenius plot of ln k *vs* 1/T over the 10%[Bmim]Cl-$CrCl_3$/SG catalyst.

Conclusion

Supported metal ionic liquid catalysts (*x*%[Bmim]Cl-$CrCl_3$/SG) using silica gel (SG) as support were successfully obtained and exploited for the production of biodiesel via esterification of PA with ML. Among various *x*%[Bmim]Cl-$CrCl_3$/SG (*x* = 5, 10, 20 and 30), the 10%[Bmim]Cl-$CrCl_3$/SG catalyst was confirmed with the best catalytic activity, excellent thermal stability and recyclability with the biodiesel yield of 96.1%. Using RSM, the obtained optimized process variables were obtained as follow: molar ratio of ML/PA = 11:1 mol/mol, catalyst amount = 5.3 wt%, time = 65 min, and temperature = 373 K. Additionally, further kinetic studies revealed that esterification of PA with ML over the 10%[Bmim]Cl-$CrCl_3$/SG catalysts followed a reaction order of 1.41 with E_a of 16.88 kJ/mol. Moreover, the application of silica gel supported metal ionic liquid catalysts effectively makes up the shortage of the high viscosity of the ionic liquid, reduces the use of ionic liquid, saves the cost of experiments, and facilitates recovery and recycling of the catalyst. These results fully demonstrate that this catalyst can replace conventional catalysts for biodiesel production.

Acknowledgement

The funding support of this work by Jiangsu Key Laboratory of Regional Resource Exploitation and Medicinal Research (No. LPRK201701) is gratefully acknowledged.

References

1 E. Atabani, A. S. Silitonga, I. A. Badruddin, T. M. I. Mahlia, H. H. Masjuki and S. Mekhilef, A comprehensive review on biodiesel as an alternative energy resource and its characteristics, *Renew. Sust. Energ. Rev*. **16**, 2070 (2012).

2 M. B. Dantas, M. M. Conceicao, Jr, V. J. Fernandes, N. A. Santos, R. Rosenhaim, A. L. B. Marques, I. M. G. Santos and A.G. Souza, Evaluation of the oxidative induction time of the ethilic castor biodiesel, *J. Therm. Anal. Calorim*. **97**, 643 (2009).

3 X. Q. Li, D. M. Tong and C. W. Hu, Efficient production of biodiesel from both esterification and transesterification over supported SO_4^{2-}-MoO_3-ZrO_2- Nd_2O_3/SiO_2 catalysts, *J. Energ. Chem*. **1**, 463 (2015).

4 A. F. Lee, J. A. Bennett, J. C. Manayil and K. Wilson, Heterogeneous catalysis for sustainable biodiesel production via esterification and transesterification, *Chem. Soc. Rev*. **43**, 7887 (2014).

5 X. X. Yang, Y. T. Wang, Y. T. Yang, E. Feng, J. Luo, F. Zhang, W. J. Yang and G. R. Bao, Catalytic transesterification to biodiesel at room temperature over several solid bases, *Energ. Convers. Manage*. **164**, 112 (2018).

6 Z. Amini, Z. Iiham, H. C. Ong, H. Mazaheri and

W. H. Chen, State of the art and prospective of lipase-catalyzed transesterification reaction for biodiesel production, *Energ. Convers. Manage*. **141**, 339 (2016).

7 Y. T. Wang, Z. Fang and F. Zhang, Esterification of oleic acid to biodiesel catalyzed by a highly acidic carbonaceous catalyst, *Catal. Today*, **319**, 172 (2018).

8 Y. R. Lee, Y. J. Lee, W. W. Ma and K. H. Row, Determination of deep eutectic solvents as eco-friendly catalysts for biodiesel esterification from an alcohol-palmitic acid mixture, *Korean J. Chem. Eng*. **33**, 2337 (2016).

9 K. Saravanan, B. Tyagi, R. S. Shukla and H. C. Bajaj, Solvent free synthesis of methyl palmitate over sulfated zirconia solid acid catalyst, *Fuel* **165**, 298 (2016).

10 C. C. J. Alípio, K. C. S. Luiz, E. F. C. Carlos, E. Longo, R. Z. José and N. R. F. Geraldo, Production of biodiesel by esterification of palmitic acid over mesoporous aluminosilicate Al-MCM-41, *Fuel* **88,** 461 (2009).

11 X. X. Han, Y. F. He, C. T. Hung, L. L. Liu, S. J. Huang and S. B. Liu, Efficient and reusable polyoxometalate-based sulfonated ionic liquid catalysts for palmitic acid esterification to biodiesel, *Chem. Eng. Sci*. **104**, 64 (2013).

12 X. X. Han, K. K. Chen, W. Yan, C. T. Hung, L. L. Liu, P. H. Wu, K. C. Lin and S. B. Liu, Amino acid-functionalized heteropolyacids as efficient and recyclable catalysts for esterification of palmitic acid to biodiesel, *Fuel* **165**, 115 (2016).

13 T. H. Đặng and B. H. Chen, Optimization in esterification of palmitic acid with excess methanol by solid acid catalyst, *Fuel Process. Technol*. **109**, 7 (2013).

14 R. Purova, K. Narasimharao, N. S. I. Ahmed, S. Al-Thabaiti, A. Al-Shehri, M. Mokhtar and W. Schwieger, Pillared HMCM-36 zeolite catalyst for biodiesel production by esterification of palmitic acid, *J. Mol. Catal. A-Chem.* **406**, 159 (2015).

15 V. C. D. Santos, K. Wilson, A. F. Lee and S. Nakagaki, Physicochemical properties of WO_x/ZrO_2 catalysts for palmitic acid esterification, *Appl. Catal. B-Environ*. **162**, 75 (2015).

16 J. M. Zhu, B. T. He, J. H. Huang, C. C. Li and T. Ren, Effect of immobilization m ethods and the pore structure on CO_2 separation performance in silica-supported ionic liquids, *Micropor. Mesopor. Mat*. **260**, 190 (2018).

17 T. Welton, Room-temperature ionic liquids. Solvents for synthesis and catalysis, *Chem. Rev*. **30**, 2071 (1999).

18 B. Aghabarari, N. Dorostkar, M. Ghiaci, S. G. Amini, E. Rahimi and M. V. Martinez-Huerta, Esterification of fatty acids by new ionic liquids as acid catalysts, *J. Taiwan Inst. Chem*. E. **45,** 431(2014).

19 Y. Y. Feng, T. Qiu, J. B. Yang, L. Li, X. D. Wang and H. X. Wang, Transesterification of palm oil to biodiesel using Brønsted acidic ionic liquid as high-efficient and eco-friendly catalyst, *Chinese J. Chem. Eng*. **25**, 1222 (2017).

20 M. M. Fan, J. J. Zhou, Q. J. Han and P. B. Zhang, Effect of various functional groups on biodiesel synthesis from soybean oils by acidic ionic liquids, *Chinese Chem. Lett*. **23**, 1107 (2012).

21 B. Zhen, Q. Z. Jiao, Q. Wu and H. H. Li, Catalytic performance of acidic ionic liquid-functionalized silica in biodiesel production, *J. Energ. Chem*. **23**, 97 (2014).

22 L. Zhang, Y. D. Cui, C. P. Zhang, L. Wang, H. Wan, G. F. Guan, Biodiesel production by esterification of oleic acid over Brønsted acidic ionic liquid supported onto Fe-incorporated SBA-15, *Ind. Eng. Chem. Res*. **51**, 16590 (2012).

23 Y. N. Sun, J. L. Hu, S. An, Q. Q. Zhang, Y. H. Guo, D. Y. Song and Q. K. Shang, Selective esterification of glycerol with acetic acid or lauric acid over rod-like carbon-based sulfonic acid functionalized ionic liquids, *Fuel*, **207,** 136 (2017).

24 A. I. Khuri and J. A. Cornell, Response surfaces: Designs and Analyses, New York, NY: Marcel Dekker. 1987.

25 K. Hinkelmann and J. Jo, Linear trend-free Box-Behnken designs, *J. Stat. Plan. Infer*. **72**, 347 (1998).

26 X. X. Han and L. X. Zhou, Optimization of process variables in the synthesis of butyl butyrate using acid ionic liquid as catalyst, *Chem. Eng. J*. **172**, 459 (2011).

27 S. H. Xun, W. H. Zhu, D. Zheng, L. Zhang, H. Liu, S. Yin, M. Zhang and H. M. Li, Synthesis of metal-based ionic liquid supported catalyst and its application in catalytic oxidative desulfurization of fuels, *Fuel* **136**, 358 (2014).

28 Y. S. Ding, F. L. Zhao, H. M. Leng, W. Zhong and S. X. Yu, Study on synthesis and chemical structures of 1-butyl-3-methylimidazolium chloride, *Appl. Chem. Ind*. **44**, 923 (2015) (in Chinese).

29 E. Rafiee and F. Mirnezami, Temperature regulated Brønsted acidic ionic liquid-catalyze esterification of oleic acid for biodiesel application, *J. Mol. Struct*. **1130**, 296 (2017).

30 S. Y. Yu, L. P. Wang, B. Chen, Y. Y. Gu, J. Li, H. M. Ding and Y. K. Shan, Assembly of heteropoly acid nanoparticles in SBA-15 and its performance as an acid catalyst, *Chem. Eur. J.* **11**, 3894 (2005).

31 H. T. Ashif, A. C. Avinash, A. S. Faheem, C. Wook-Jin and K. Hern, Synthesis, characterization, and application of silica supported ionic liquid as catalyst for reductive amination of cyclohexanone with formic acid and triethyl amine as hydrogen source, *Chinese J. Catal*. **36**, 1365 (2015).

32 F. Zhang, Z. Fang and Y. T. Wang, Biodiesel production directly from oils with high acid value by magnetic Na_2SiO_3@Fe_3O_4/C catalyst and ultrasound, *Fuel*, **150**, 370 (2015).

33 T. Long, Y. Deng, S. Gan and J. Chen, Application of choline chloride·$x$$ZnCl_2$ ionic liquids for preparation of biodiesel, *Chinese J. Chem. Eng*. **18**, 322 (2010).

34 Y. Q. Wang, D. Zhao, L. L. Wang, X. Q. Wang, L. J. Li, Z. P. Xing, N. Ji, S. J. Liu and H. Ding, Immobilized phosphotungstic acid based ionic liquid: Application for heterogeneous esterification of palmitic acid, *Fuel*, **216**, 364 (2018).

35 K. Saravana, B. Tyagi, R. S. Shukla and H. C. Bajaj, Esterification of palmitic acid with methanol over template-assisted mesoporous sulfated zirconia solid acid catalyst, *Appl. Catal. B-Environ*. **172**, 108 (2015).

36 S. A. Fernandes, R. Natalino, M. J. D. Silva and C. F. Lima, A comparative investigation of palmitic acid esterification over *p*-sulfonic acid calix[4] arene and sulfuric acid catalysts via H-1 NMR spectroscopy, *Catal. Commun*. **26**, 127 (2012).

37 K. Srilatha, N. Lingaiah, B. L. A. Prabhavathi Devi, R. B. N. Prasad, S. Venkateswar and P. S. Sai Prasad, Esterification of free fatty acids for biodiesel production over heteropoly tungstate supported on niobia catalysts, *Appl. Catal. A-Gen*. **365**, 28 (2009).